$Ba_2Cu_{18-x}As_{10}$: A New Mixed-Valent Ternary Copper-Rich Arsenide with Metallic Properties

Sung-Jin Kim,[†,‡] John Ireland,[§] Carl R. Kannewurf,[§] and Mercouri G. Kanatzidis*[,†]

Department of Chemistry and Center for Fundamental Materials Research, Michigan State University, East Lansing, Michigan 48824, and Department of Electrical Engineering and Computer Science, Northwestern University, Evanston, Illinois 60208

Received February 18, 2000. Revised Manuscript Received July 11, 2000

The new barium copper pnictide $Ba_2Cu_{18-x}As_{10}$ ($x \approx 1.67$) was obtained from a direct element combination reaction in a sealed graphite tube at 700 °C, and its structure was determined by single-crystal X-ray diffraction methods. It crystallizes in the trigonal space group $P\bar{3}1c$ (No. 163) with $a = 6.7329(1)$ Å, $c = 11.6747(2)$ Å, and $Z = 1$. $Ba_2Cu_{18-x}As_{10}$ has a three-dimensional structure with straight bottle-shape parallel tunnels running along the *c*-direction. The Ba atoms reside in the tunnels. The $[Cu_{18-x}As_{10}]^{4-}$ framework features Cu atom vacancies with $x = 1.67$. The compound is metallic with a room-temperature resistivity along the *c*-axis of 1.7×10^{-4} Ω·cm and a Seebeck coefficient of ~+2.5 μV/K. Band structure calculations in the extended Hückel approximation suggest that the defects on the Cu sites enhance its metallic character.

Introduction

Ternary metal-rich alkaline earth transition metal pnictides can be considered to be at the borderline between Zintl and intermetallic phases.[1] The bonding aspects of these borderline phases often show so-called "locally delocalized electrons". However, their structures and bonding of this group of compounds only recently began to be seriously investigated. In ternary barium copper arsenides several compounds such as $Ba_2Cu_{1.88}As_2$,[2] $BaCu_6As_2$,[3] ACu_4As_2 (A = Ca, Ba, Eu),[4] BaCuAs,[5] and $BaCu_8As_4$[6] are known along with their analogous phosphides.[1e,f] The most frequent structure type for ternary transition metal compounds is the tetragonal $ThCr_2Si_2$ type.[7] For example, $CaCu_2As_2$ crystallizes in this structure,[1e] where $CuAs_4$ tetrahedra are edge-shared to form layers, which in turn are connected with As−As bonds to form a three-dimensional network. The compounds of the $ThCr_2Si_2$ type can be rationalized with Zintl's concept.[2] Some derivatives of $ThCr_2Si_2$ structure type have vacancies on Cu sites as for example $Ba_2Cu_3P_4$ (≃$BaCu_{1.50}P_2$) and $BaCu_{1.88}As_2$.[2] In the copper-rich region the compounds form extensive Cu−Cu bonds as observed in $BaCu_6As_2$ and $BaCu_8As_4$. The $BaCu_6As_2$ can be described as an intergrowth of $ThCr_2Si_2$ and Cu structure-type segments.[3] In $BaCu_8As_4$ a three-dimensional $[Cu_8As_2]^{2-}$ network forms two types of tunnels with different diameters, where Ba^{2+} atoms and infinite chains of edge-shared Cu_4 tetrahedra are respectively situated.[6] ACu_4As_2 (A = Ca, Ba, Eu) have a layered structure, where the copper atoms are tetrahedral and nearly trigonal planar.[4] BaCuAs is also layered and adopts the Ni_2In-type structure.[5]

Here, we describe a new member of this family, $Ba_2Cu_{18-x}As_{10}$, discovered during attempts to synthesize the arsenic analogue of the clathrate-type compound $Ba_8Cu_{16}P_{30}$.[8] The new compound exhibits a new structure type and possesses metallic properties deriving from mixed valency of the Cu and As atoms. There are two known related clathrate-type phosphides, $Ba_8Cu_{16}P_{30}$ and $BaCu_2P_4$,[9] where three-dimensionally linked CuP_4 tetrahedra form large open cavities filled with Ba atoms. $Ba_8Cu_{16}P_{30}$ is an orthorhombic derivative of typical clathrate-I.[8] $BaCu_2P_4$ consists of infinite helical chains of clathrate-type cages. Our interest in the copper arsenides with possible clathrate structures and semiconducting properties derives from their possible relevance to thermoelectrics research.[10,11]

* To whom correspondence should be addressed. E-mail: Kanatzid@cem.msu.edu. Tel: 517-353-0174.
† Michigan State University.
‡ Permanent address: Department of Chemistry, Ewha Woman's University, Seoul, Korea, #120-750.
§ Northwestern University.

(1) (a) Nesper, R. *Angew. Chem., Int. Ed. Engl.* **1991**, *30*, 789. (b) Miller, G. J. *Chemistry, Structure, and Bonding of Zintl Phases and Ions*; Kauzlarich, S. M., Ed.; VCH Publishers: New York, 1996; p1. (c) von Schnering, H. G. *Angew. Chem., Int. Ed. Engl.* **1981**, *20*, 33. (d) Young, D. M.; Charlton, J.; Olmstead, M. M.; Kauzlarich, S. M.; Lee, C.-S.; Miller, G. J. *Inorg. Chem.* **1997**, *36*, 2539. (e) Pilchowski, I.; Mewis, A. *Z. Anorg. Allg. Chem.* **1990**, *581*, 182. (b) Mewis, A. *Z. Naturforsch.* **1980**, *35b*, 141. (f) Pfisterer, M.; Nagorsen, G. *Z. Naturforsch.* **1980**, *35b*, 703.
(2) Dünner, J.; Mewis, A.; Roepke, M.; Michels, G. *Z. Anorg. Allg. Chem.* **1995**, *621*, 1523.
(3) Dünner, J.; Mewis, A. *J. Alloys Compd.* **1995**, *221*, 65.
(4) (a) Dünner, J.; Mewis, A. *Z. Anorg. Allg. Chem.* **1999**, *625*, 625. (b) Pfisterer M.; Nagorsen Günter *Z. Naturforsch.* **1982**, *37b*, 420.
(5) (a) Mewis, A. Blumstengel, P. *Z. Naturforsch.* **1978**, *33b*, 671. (b) Mewis, A. *Z. Naturforsch.* **1978**, *33b*, 983. (c) Mewis, A. *Z. Naturforsch.* **1979**, *34b*, 1373.
(6) Pilchowski, I.; Mewis, A.; Wenzel, M.; Gruehn, R. *Z. Anorg. Allg. Chem.* **1990**, *588*, 109.
(7) (a) Andress K. R.; Alberti, E. *Z. Metallkd.* **1935**, *27*, 126. (b) Zheng, C.; Hoffmann, R. *Z. Naturforsch.* **1986**, *41b*, 292. (c) Eisenmann, B.; May, N.; Müller, W. Schäfer, H. *Z. Naturforsch.* **1972**, *27b*, 1155.
(8) Dünner, J.; Mewis, A. *Z. Anorg. Allg. Chem.* **1995**, *621*, 191.
(9) Dünner, J.; Mewis, A. *J. Less-Common Met.* **1990**, *167*, 127.

10.1021/cm0001455 CCC: $19.00
Published on Web 09/23/2000

Experimental Section

Synthesis. $Ba_2Cu_{18-x}As_{10}$ was first identified in a reaction intended to synthesize a new clathrate-type analogue with $Ba_8Cu_{16}As_{30}$ composition. The crystal used in the structure determination resulted from the reaction of a mixture of three elements (Ba, Aldrich, chunk under oil, 99%; Cu, Cerac, powder, 99.999%; As, Cerac, powder, 99.999%) in a molar ratio of 8:16:30. The reaction mixture was placed in a graphite tube and sealed in an evacuated silica tube. The sealed mixture was heated slowly up to 700 °C, kept at that temperature for 1 day, and subsequently cooled to room temperature over 1 day. The reaction led to the formation of black bar-shaped or triangular-shaped crystals along with gray powder. The X-ray powder diffraction pattern indicated the product was a mixture of $Ba_2Cu_{18-x}As_{10}$ and Ba_3As_{14}. Semiquantitative microprobe analysis on single crystals gave $Ba_{2.0(2)}Cu_{15.52(2)}As_{9.88(2)}$ (average of three data acquisitions). Once the stoichiometry was determined from the X-ray single-crystal structure analysis, pure $Ba_2Cu_{18-x}As_{10}$ was prepared starting from the exact stoichiometric ratio of the elements. When excess arsenic was used, silvery bar-shaped crystals and unreacted arsenic chunks were obtained. The X-ray powder diffraction pattern of the bulk product agreed well with the powder pattern calculated from the single-crystal data.

Electron Microscopy. Semiquantitative microprobe analysis of the compounds was performed with a JEOL JSM-35C scanning electron microscope (SEM) equipped with a Tracor Northern energy dispersive spectroscopy (EDS) detector. Data were acquired using an accelerating voltage of 20 kV and a 30-s accumulation time. The results reported are an average of multiple measurements done on several single crystals of a given compound.

Electronic Structure Calculations. Electronic structure calculations were performed by the Hückel method within the framework of the tight-binding approximation.[12] The program CAESAR for IBM-compatible PC was used.[13] Density of states (DOS) were calculated on the basis of the 216 k points set of the trigonal structure.

Charge-Transport Measurements. DC electrical conductivity and thermopower measurements were made on a single crystal with ~2 mm length and ~0.1 mm diameter. Conductivity measurement was performed in the usual four-probe geometry with 60- and 25-μm gold wires used for the current and voltage electrodes, respectively. Measurements of the sample cross-sectional area and voltage probe separation were made with a calibrated binocular microscope. Conductivity data were obtained with the computer-automated system described elsewhere.[14a] Thermoelectric power measurements were made by using a slow ac technique[14b] with 60-μm gold wires serving to support and conduct heat to the sample, as well as to measure the voltage across the sample resulting from the applied temperature gradient. In both measurements, the gold electrodes were held in place on the sample with a conductive gold paste.

Conductivity specimens were mounted on interchangeable sample holders, and thermopower specimens were mounted on a fixed sample holder/differential heater. Mounted samples were placed under vacuum (10^{-3} Torr) and heated to room temperature for 2−4 h to cure the gold contacts. For a variable-temperature run, data (conductivity or thermopower) were acquired during both sample cooling and warming to check reversibility. The temperature drift rate during an experiment was kept below 1 K/min. Typically, three to four separate variable-temperature runs were carried out for each sample to ensure reproducibility and stability. At a given temperature, reproducibility was within ±5%.

Crystallographic Studies. A silvery triangular-shaped crystal with dimensions of 0.02 × 0.02 × 0.05 mm^3 was mounted on a glass fiber. A Siemens SMART Platform CCD diffractometer was used to collect intensity data using graphite monochromatized Mo Kα radiation. The data were collected over a full sphere of reciprocal space up to 56° in 2θ. The individual frames were measured with a ω rotation of 0.3° and an acquisition time of 30 s. The SMART software[15] was used for data acquisition, and SAINT,[16] for data extraction and reduction. The absorption correction was performed empirically using SADABS.[17] The unit cell parameters were obtained from least-squares refinement using randomly chosen 600 reflections from a full sphere of reciprocal space up to 56° in 2θ. The observed Laue symmetry and systematic extinctions were indicative of the space group $P\bar{3}1c$ and $P31c$. The centrosymmetric $P\bar{3}1c$ was assumed, and subsequent refinements confirmed the choice of this space group. The initial positions of all atoms were obtained with direct methods. The structure was refined with full-matrix least-squares techniques with the SHELXTL[18] package of crystallographic programs. The ideal formula based on the crystallographic determination was $Ba_2Cu_{18}As_{10}$. Once all atoms were located, the temperature factors of Cu(2) and As(2) were found to be relatively large. When the occupancy of Cu(2) was allowed to vary, it dropped to the value of 55.7(8)%. The possibility of placing As atoms on Cu(2) sites was considered, but it was excluded on the basis of the final refinement and composition obtained from EDX analysis. When the occupancy of As(2) sites was allowed to vary, the refinement did not lead to any significant change in the occupation factor. The final cycle of refinement performed on F_o^2, with 27 variables and 379 averaged reflections, converged to residuals wR2 ($F_o^2 > 0$) = 0.070. On the other hand, the conventional R index based on reflections having $F_o^2 > 2\sigma(F_o^2)$ was 0.0299. A difference Fourier synthesis map calculated with phases based on the final parameters showed maximum and minimum peaks of 2.65 and −2.17 e/Å^3 at 0.17 and 0.86 Å from As(2), respectively. The complete data collection parameters and details of structure solution and refinement results are given in Table 1. Final atomic positions and anisotropic displacement parameters are given in Tables 2 and 3.

To check the possibility of a superstructure, due to vacancy ordering, an electron diffraction study was performed on several crystals at room temperature. No evidence of superstructure was indicated on the electron diffraction photographs. In addition, a careful X-ray diffraction study at low temperature (173 K) along every crystal axis did not reveal superstructure reflections.

Results and Discussion

Structure. The compound $Ba_2Cu_{18-x}As_{10}$ has a new structure type with extensive Cu−Cu bonding and cylindrical tunnels knitted with Cu and As atoms. This structure is related to that of $BaNi_9P_5$ except for a slight difference in space group symmetries and metal atom vacancies.[19] The projection along the *c* axis shows hexagonal tube-shape tunnels filled with Ba atoms,

(10) (a) Nolas, G. S.; Cohn, J. L.; Slack, G. A.; Schujman, S. B. *Appl. Phys. Lett.* **1998**, *73*, 178. (b) Nolas, G. S.; Cohn, J. L.; Slack, G. A. *Phys. Rev.* **1998**, *B58*, 164. (c) Nolas, G. S.; Weakley T.; Cohn, J. L. *Chem. Mater.* **1999**, *11*, 2470.

(11) (a) Sales, B. C.; Chakoumakos, B. C.; Mandrus, D.; Sharp, J. W. *J. Solid State Chem.* **1999**, *146*, 528. (b) Blake, N. P.; Mollnitz, L, Kresse, G.; Metiu, H. *J. Chem. Phys.* **1999**, *111*, 3133.

(12) (a) Hoffman, R. *J. Chem. Phys.* **1963**, *39*, 1397. (b) Whangbo, M.-H.; Hoffmann, R.; Woodward, R. B. *Proc. R. Soc. London* **1979**, *A366*, 23.

(13) Ren, J.; Liang, W.; Whangbo, M.-H. Primecolor Software, Inc., Cary, NC, **1999**.

(14) (a) Lyding, J. W.; Marcy, H. O.; Marks, T. J.; Kannewurf, C. R. *IEEE Trans. 1nstrum. Meas.* **1988**, *37*, 76. (b) Marcy, H. O.; Marks, T. J.; Kannewurf, C. R. *IEEE Trans. Instrum. Meas.* **1990**, *39*, 756.

(15) SMART: Siemens Analytical X-ray Systems, Inc., Madison, WI, 1994.

(16) SAINT, Version 4: Siemens Analytical X-ray Systems, Inc., Madison, WI, 1994.

(17) Sheldrick, G. M. University of Göttingen, Göttingen, Germany, to be published.

(18) Sheldrick, G. M. *SHELXTL, Version 5*; Siemens Analytical X-ray Systems, Inc.: Madison, WI, 1994.

(19) Badding, J. V.; Stacy, A. M. *J. Solid State Chem.* **1990**, *87*, 10.

Table 1. Selected Data from the Single-Crystal Refinement of $Ba_2Cu_{18-x}As_{10}$

empirical formula	$Ba_2Cu_{18-x}As_{10}$
fw	1997.95
temp (K)	173(2)
wavelength (λ =Kα, Å)	0.71073
cryst system	Trigonal
space group	$P\bar{3}1c$ (No. 163)
unit cell dimens (Å)	a = 6.7329(1)
	c = 11.6747(2)
V (Å^3)	458.332(12)
Z	1
density, ρ_{calc} (g/cm^3)	7.239
abs coeff (mm^{-1})	39.461
reflcns collcd	4269
data/restraints/params	379/0/27
final R indices [$F_o^2 > 2\sigma(F_o^2)$][a]	R1 = 0.0299, wR2 = 0.0693
R indices ($F_o^2 > 0$)	R1 = 0.0320, wR2 = 0.0702
Largest diff peak and hole (e Å^{-3})	2.653 and −2.017

[a] R1 = $[\sum||F_o| - |F_c||]/\sum|F_o|$. wR2 = $\{[\sum w(|F_o| - |F_c|)^2/[\sum w(F_o^2)^2]]\}^{1/2}$. $w = \sigma_F^{-2}$.

Table 2. Atomic Coordinates (×10^4) and Equivalent Isotropic Displacement Parameters (Å^2 × 10^3) for $Ba_2Cu_{18-x}As_{10}$[a]

atom	Wyckoff symbol	x	Y	z	U(eq)[a]
Ba(1)	2b	0	0	0	10(1)
Cu(1)	12i	5374(2)	749(2)	1065(1)	10(1)
Cu(2)[b]	6h	5709(1)	7854(2)	2500	13(1)
As(1)	4f	3333	6667	650(1)	6(1)
As(2)	6h	2990(3)	1495(2)	2500	32(1)

[a] U(eq) is defined as one-third of the trace of the orthogonalized U_{ij} tensor. [b] Occupancy is 0.557(8).

Table 3. Anisotropic Displacement Parameters (Å^2 × 10^3)[a] for $Ba_2Cu_{18-x}As_{10}$

atom	U_{11}	U_{22}	U_{13}	U_{33}	U_{23}	U_{12}
Ba(1)	12(1)	12(1)	7(1)	0	0	6(1)
Cu(1)	12(1)	7(1)	9(1)	0	0(1)	3(1)
Cu(2)[b]	13(1)	14(1)	10(1)	0(1)	0	6(1)
As(1)	6(1)	6(1)	6(1)	0	0	3(1)
As(2)	28(1)	55(1)	4(1)	0(1)	0	14(1)

[a] The anisotropic displacement factor exponent takes the following form: $-2\pi^2[h^2a^{*2}U_{11} + ... + 2hka^*b^*U_{12}]$. [b] Occupancy is 0.557(8).

Figure 1. The 3-fold rotoinversion $\bar{3}$ axes are running through the Ba atoms in the center of the tunnels. The basic building blocks of the $[Cu_{18-x}As_{10}]^{4-}$ framework are shown in Figure 2. Hexanuclear trigonal prisms of Cu, capped with five As atoms, stack along the c axis to form straight infinite columns. A 3-fold axis passes through each column. The columns are linked side-by-side to form the three-dimensional structure, and the nearest-neighbor columns are related to each other with crystallographic c glides. A scheme of two-column condensation is shown in Figure 2. Overall, six columns are condensed to form one tunnel. Selected bond distances are listed in Table 4.

In Figure 3a,b, the two building blocks that form each chain are shown in greater detail with bond distances and labels. The elementary building block is a capped copper trigonal prism and As-centered trigonal prisms of copper atoms. The Cu(1)−Cu(1) distances in the trigonal plane are 2.610(2) Å, which is slightly longer than that observed in bulk Cu metal (2.56 Å)[20] and comparable to the distance observed in other ternary

(20) Straumanis, M. E.; Yu, L. S. *Acta Crystallogr., Sect. A* **1969**, *25A*, 676.

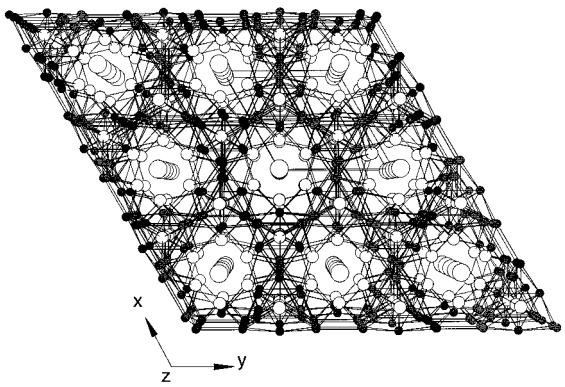

Figure 1. (a) A [001] view of the trigonal unit cell of $Ba_2Cu_{18-x}As_{10}$. The Ba, Cu, and As atoms are indicated by large open circles, small filled, and small open circles, respectively.

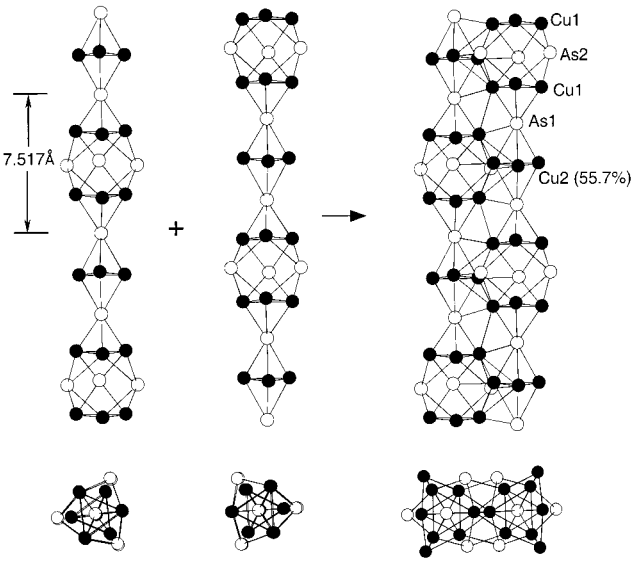

Figure 2. Scheme of two-column condensation with atomic labeling. The columns are shown along the c axis at the top. Projections down the c-axis are shown at the bottom. The lengths of hexanuclear trigonal prisms of Cu are capped with five As atoms.

copper arsenides. The Cu−Cu bond distances in $BaCu_8As_4$ and $BaCu_6As_2$ are in a range of 2.476(1)−2.719(1) and 2.559−2.978(1) Å, respectively.

In $Ba_2Cu_{18-x}As_{10}$, the bond distance between Cu(1)−As(2) is 2.539(1) Å, comparable to the distances observed in other ternary barium copper arsenides. For example, the bond distances between Cu and As atoms are in a range of 2.411−2.595 Å in $BaCu_8As_4$ and $BaCu_6As_2$. The local coordination environment of Cu(1) and Cu(2) is a very distorted tetrahedron of As atoms; see Table 4 for angles. However both Cu atoms have several additional neighbor Cu atoms at distances between 2.400 and 2.664 Å. Figure 3b shows the As-centered copper antiprism waisted by three Cu(1) atoms (labeled as Cu1′) from neighboring chains. The bond distances between the centered As(1) and the waisted three Cu(1) atoms are 2.429(1) Å, and those between As(1) and Cu(2) are 2.565(2) Å. The Cu(2)−Cu(2) bond distance is 2.400(5) Å, which is much shorter than those of Cu(1)−Cu(1) at 2.611(2) Å. One of the shortest Cu−Cu distances reported is 2.450 Å in $BaCu_{10}P_4$.[1d] The single covalent metallic distance of copper is 2.34 Å,[21] and the Cu−Cu distance in bulk metal is 2.56 Å.[20] Despite the partial

Table 4. Selected Bond Distances (Å) and Angles (deg) in $Ba_2Cu_{18-x}As_{10}$

Ba(1)−As(2) (×6)	3.3996(9)	Cu(1)−Cu(1) (×2)	2.6102(16)
Ba(1)−Cu(1) (×6)	3.6147(10)	Cu(1)−Cu(1)	2.6347(19)
Ba(1)−Cu(2)	3.8442(17)	Cu(1)−Cu(2) (×2)	2.6636(10)
As(1)−Cu(1) (×3)	2.4288(10)	Cu(2)−As(2) (×2)	2.222(2)
As(1)−Cu(1) (×3)	2.5062(14)	Cu(2)−Cu(2) (×2)	2.400(5)
As(1)−Cu(2) (×3)	2.5652(18)		
Cu(1)−As(2)	2.5385(14)		
Cu(1)−As(2)	2.5390(14)		
Cu(1)−As(1)−Cu(1)	116.14(2)	As(2)−Cu(2)−Cu(1)	61.84(4)
Cu(1)−As(1)Cu(1)	64.51(4)	Cu(2)−Cu(2)−Cu(1)	63.24(6)
Cu(1)−As(1)−Cu(1)	116.99(5)	Cu(2)−Cu(2)−Cu(1)	108.87(6)
Cu(1)−As(1)−Cu(1)	62.76(4)	As(1)−Cu(2)−Cu(1)	55.31(3)
Cu(1)−As(1)−Cu(2)	64.40(3)	As(1)−Cu(2)−Cu(1)	119.34(6)
Cu(1)−As(1)−Cu(2)	111.21(7)	Cu(1)−Cu(2)−Cu(1)	77.97(4)
Cu(1)−As(1)−Cu(2)	120.68(5)	Cu(1)−Cu(2)−Cu(1)	101.40(4)
Cu(1)−As(1)−Cu(2)	175.72(6)	Cu(1)−Cu(2)−Cu(1)	171.58(12)
Cu(2)−As(1)−Cu(2)	55.77(8)	As(1)−Cu(2)−As(1)	85.60(12)
Cu(2)−As(2)−Cu(2)	154.40(13)	As(1)−Cu(2)−Cu(2)	107.20(6)
Cu(2)−As(2)−Cu(1)	67.67(4)	As(1)−Cu(2)−As(1)	113.34(3)
Cu(2)−As(2)−Cu(1)	128.51(4)	Cu(2)−Cu(2)−As(1)	62.11(4)
Cu(1)−As(2)−Cu(1)	113.58(8)		
Cu(1)−As(2)−Cu(1)	82.61(5)		
Cu(1)−As(2)−Cu(1)	61.87(5)		
As(1)−Cu(2)−As(1)	114.62(10)	As(2)−Cu(1)−Cu(1)	102.56(4)
As(1)−Cu(2)−Cu(1)	125.41(8)	As(2)−Cu(1)−Cu(1)	132.83(7)
Cu(2)−Cu(2)−Cu(1)	108.88(6)	Cu(1)−Cu(1)−Cu(1)	106.67(5)
As(1)−Cu(2)−Cu(1)	119.34(6)	As(1)−Cu(1)−Cu(2)	60.29(5)
As(1)−Cu(2)−Cu(1)	55.32(3)	As(2)−Cu(1)−Cu(2)	50.50(6)
As(1)−Cu(2)−Cu(1)	61.83(4)	As(2)−Cu(1)−Cu(2)	91.30(4)
Cu(2)−Cu(2)−Cu(1)	63.24(6)	Cu(1)−Cu(1)−Cu(2)	140.70(2)
Cu(1)−Cu(2)−Cu(1)	171.60(12)	Cu(1)−Cu(1)−Cu(2)	108.89(7)
As(1)−Cu(1)−As(1)	115.49(4)	Cu(1)−Cu(1)−Cu(2)	112.56(5)
As(1)−Cu(1)−As(2)	107.42(5)	Cu(2)−Cu(1)−Cu(2)	53.54(11)
As(2)−Cu(1)−As(2)	94.01(6)		
As(1)−Cu(1)−Cu(1)	148.05(6)		
As(1)−Cu(1)−Cu(1)	58.62(2)		

occupancy of Cu(2), the bond length of Cu(2)−Cu(2) seems comparable to the single covalent metallic bond distance of copper (2.34 Å). However, the nearest atoms from the Cu(2) to As(2) are at 2.222(2) Å, which seems to be too short for a normal As−Cu bond length. As(2) and Cu(2) atoms are both located at a special 6h position with 2-fold symmetry at (*x*, *y*, 1/4). The atomic displacement parameters of As(2) atoms are three times larger than those of the other atoms in the structure, which seems to be related to the partial occupancy on the Cu(2) sites. The latter gives rise to the artificially short Cu(2)−As(2) distances. The dynamic nature of the strong anisotropic displacement of As(2) atoms in the *ab* plane strongly suggests that these atoms shift toward the vacant sites of Cu(2), Figure 3c. The nonstoichiometric composition $Ba_2Cu_{18-x}As_{10}$ raises the question of a superstructure due to vacant site ordering; however, such was not found. The structure solution with random disorder on Cu(2) sites seems to be the best description of the structure of $Ba_2Cu_{18-x}As_{10}$. It may also have implications for Cu-ion mobility in this material.

Figure 4a illustrates the coordination around the Ba atoms along the *c*-axis direction, and Figure 4b is the projected view showing the shape of the open channel with Ba atoms reside. The Ba-centered cage is constructed from two layers of Cu atoms and two layers of As atoms stacked to form infinite bottle-shaped channels running along the *c*-axis direction. Six As atoms form a pseudooctahedral pocket which is elongated along the *c* axis. This pocket accommodates a Ba^{2+} cation with Ba−As distances of 3.3996(9) Å. This makes a narrow passage in the tunnel acting as a bottleneck. The next nearest atoms from Ba are 12 Cu(1) atoms at 3.615(1) Å on two layers, which form the wider part of the channel.

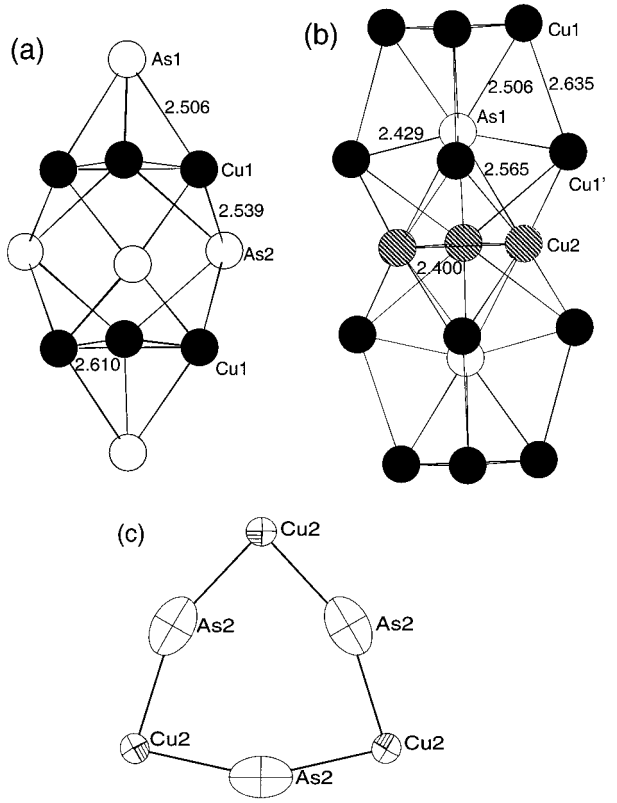

Figure 3. (a) Building block of capped copper trigonal prism. (b) Two As-centered trigonal antiprisms with bond lengths. (c) ORTEP representation showing interactions of As(2) and Cu(2) atoms on the *ab* plane with 80% probability thermal ellipsoids.

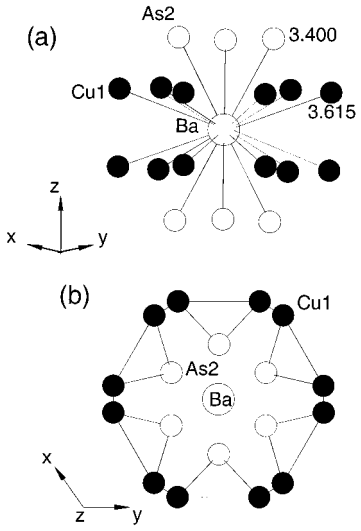

Figure 4. (a) Coordination of the Ba atom with bond lengths. (b) Projection of Ba-centered cage along the *c*-axis direction.

Charge Transport Properties. The electrical resistivity was measured on single crystals along the *c* axis as a function of temperature, Figure 5. The resistivity is very low and decreases with falling temperature suggesting metallic behavior. The room-temperature resistivity is 1.7×10^{-4} Ω·cm. The metallic behavior observed is attributed to the extensive Cu−

(21) Pauling, L. *The Nature of the Chemical Bond*; Cornell Press: Ithaca, NY, 1960; p 256.

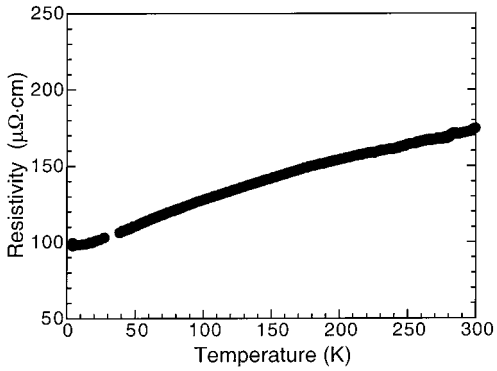

Figure 5. Temperature dependence of the electrical resistivity for a single crystal of $Ba_2Cu_{18-x}As_{10}$.

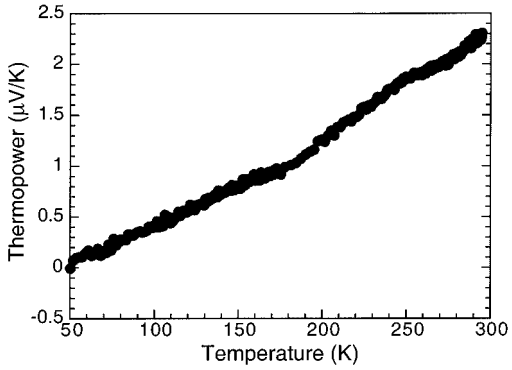

Figure 6. Temperature dependence of the thermoelectric power (Seebeck coefficient) for a single crystal of $Ba_2Cu_{18-x}As_{10}$.

Table 5. Atomic Orbital Parameters[a] Used in Extended Hückel Calculations

atom	orbital	H_{ii} (eV)[a]	ζ_1[b]	C_1[b]	ζ_2	C_2
Cu	4s	−11.40	2.20			
	4p	−6.06	2.20			
	3d	−14.00	5.95	0.5933	2.30	0.5744
As	4s	−16.22	2.23			
	4p	−12.16	1.89			

[a] $H_{ii} = \langle\chi_i|H^{eff}|\chi_i\rangle$, i = 1, 2, 3, ..., the value approximated by valence-state ionization potential. Wolfsberg, M.; Helmholz, L. *J. Chem. Phys.* **1952**, *20*, 837. [b] Single-ζ STO's. Ballhausen, C. J.; Gray, H. B. *Molecular Orbital Theory*; Benjamin: New York, 1965.

Cu bonding along the *c* axis, to the mixed valency, and to the vacancies on the Cu(2) sites.

The value of thermoelectric power (Seebeck coefficient) was ∼+2.5 μV/K at room temperature, and it shows a linear decrease with decreasing temperature, Figure 6. This behavior and the very small magnitude are typical of good metals. The positive thermoelectric power indicates that the dominant carriers are holes.

Electronic Structure. The metallic properties of the material are confirmed by the extended Hückel calculations. Assuming a rigid model, the band calculations were performed on the anionic $(Cu_{18}As_{10})^{4-}$ framework of hypothetical stoichiometry $Ba_2Cu_{18}As_{10}$. The atomic orbital parameters employed in the calculation are listed in Table 5. Figure 7 shows the total density of state (DOS) of $(Cu_{18}As_{10})^{4-}$ unit together with the orbital projections of Cu and As atoms. The Fermi level at −9.76 eV corresponds to that of the ideal composition $(Cu_{18}As_{10})^{4-}$, and that at −12.34 eV is estimated for $(Cu_{15.33}As_{10})^{4-}$. For both compositions, the Fermi levels fall in the valence band suggesting metallic behavior. The broad valence band near the Fermi level has almost

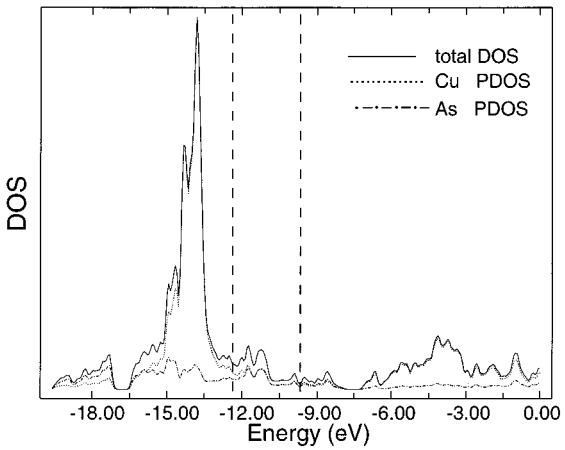

Figure 7. Density of states of $(Cu_{18}As_{10})^{4-}$. The individual atomic contributions to the total DOS are shown. The two Fermi levels marked by dashed lines at −9.76 and −12.34 eV are Fermi levels for $(Cu_{18}As_{10})^{4-}$ and $(Cu_{15.33}As_{10})^{4-}$, respectively.

equal contributions from Cu and As atoms, which indicates significant covalency in Cu−As bonds. In $(Cu_{18}As_{10})^{4-}$, the Fermi level occurs just below the band gap at nonzero minimum. This suggests that the Cu vacancies are not needed for the compound to have metallic properties. However, in the copper deficient $(Cu_{15.33}As_{10})^{4-}$, the Fermi level is situated in a region of higher density of states, which presumably serves to enhance the metallic properties. In both stoichiometric and nonstoichiometric cases, the material is not a Zintl phase. Certainly, the presence of Cu vacancies will slightly modify the details of the true band structure. Modeling vacancies in these calculations was not possible due to the limitation of the method used.

With a simple bonding model, we can qualitatively rationalize the formation of vacancies in this compound. If Cu atoms are in the +1 oxidation state, they are in the d^{10} system with empty 4s and 4p states. In ideal stoichiometric composition, both the bonding and antibonding states should be filled, which might create an unfavorable situation to hold the structure. However, the filling of the antibonding states can be avoided by the formation of vacancies on the Cu sites. A similar simple bonding model was applied to rationalize why $CaNi_2P_2$ is stable without vacancies, but the corresponding copper compound $CaCu_{1.75}P_2$ needs vacancies.[22] Both compounds, $CaNi_2P_2$ and $CaCu_{1.75}P_2$, are metallic with the $ThCr_2Si_2$-type structure.

Assuming ionic bonding, formal oxidation states can be expressed as $(Ba^{2+})_2(Cu_{15.33})^{26+}(As^{3-})_{10}$, which suggests mixed-valent states for the copper atoms. Because the As atoms are isolated from each other (no As−As interactions), their formal charge can be assigned as −3 giving an average Cu oxidation state of +1.70. However alternatively the electron distribution can be suggested as $(Ba^{2+})_2(Cu^+)_{15.33}(As_{10})^{19.33-}$ assuming Cu^+. Then the average oxidation state of As is −1.933 and the mixed valency falls on arsenic. Considering the relatively low electronegativity of As atoms, and low-lying Cu d band, a formal oxidation state of +1 for Cu atom seems to be more reasonable. In other words, electrons are expected

(22) Jeitschko, W.; Reehuis, M. *J. Phys. Chem. Solids* **1987**, *48*, 667.

to flow back to Cu d orbitals from the As p band forming Cu^{+} and As^{x-} ($x < 3$). The assumption that As atoms are not fully reduced to the As^{3-} state is consistent with the observed positive thermoelectric power.

Acknowledgment. Financial support from DARPA through the Army Research Office (Grant DAAG55-97-1-0184) and the Center for Fundamental Materials Research are gratefully acknowledged. S.-J.K. also acknowledges financial support from the MOST of Korea through Women's University.

Supporting Information Available: Tables of X-ray crystallographic data. This material is available free of charge via the Internet at http://pubs.acs.org.

CM0001455